University of Warsaw
Faculty of Economic Sciences

Norbert Jaworski
Album Number: 474891

Spatial Herfindahl-Hirschman Index (sHHI): A New Density-Aware Market Competition Index Separating Inter-Type Rivalry from Intra-Type Cannibalisation

Master's degree thesis
Field of study: Data Science and Business Analytics

The thesis written under the supervision of

dr hab. Tomasz Kopczewski

PhD Ewa Weychert

from Faculty of Economic Sciences

WNE UW

Warszawa, czerwiec 2026

TABLE OF CONTENTS

SCIENTIFIC ARTICLE

Introduction

Measuring market power without reference to space works reasonably well in industries where products and customers are mobile or markets are national in scope. It works much less well in urban services, where access is inherently local, customers are tied to neighbourhoods, and firms compete through where they place their units. Standard concentration metrics such as the Herfindahl–Hirschman Index (HHI) compress market structure into a single number by aggregating shares across firms, but they treat the economy as if it were placeless and populations as if they were uniformly smeared over a map (Hirschman, 1945; Herfindahl, 1950). In cities, neither assumption holds. People cluster; travel costs are asymmetric; small siting changes alter who wins a given street corner. An index that ignores spatial structure can therefore understate dominance in dense pockets and overstate rivalry in sparse ones. In short, if the question is "who serves whom, and where?", a density-aware, spatially explicit metric is needed.

The case for density is straightforward. A square kilometre in a high-rise district does not represent the same potential demand as a square kilometre of parkland. Two brands can operate the same number of units and yet capture very different effective market shares if one brand happens to cover a handful of dense blocks. Likewise, two cities with the same number of units per capita can exhibit sharply different competitive conditions because their people are distributed differently in space. A spatial index should, at minimum, (i) allocate potential demand to nearby units in a transparent way and (ii) weight territorial claims by people rather than land area. Only then does a concentration measure reflect the actual geometry of access.

On this point, ecology provides both language and tools. For decades, ecologists have treated space as a first-class determinant of interaction. Individuals occupy territories, compete more intensely with neighbours, and adjust survival to local crowding. A workhorse of this literature is the Voronoi (Dirichlet) tessellation, which partitions a habitat into zones of influence: each location is assigned to its nearest individual (Aurenhammer, 1991; Okabe et al., 2000). This simple geometric device turns qualitative proximity into a measurable map of inter- and intra-specific rivalry (Wiegand & Moloney, 2014). Translating that idea to urban markets is natural. Replace organisms with units (a store, a clinic, a school), and replace nutrients with population density (or age-specific need, income, etc.). The resulting cells formalise "who is closest to whom" and let us compute demand-weighted shares that respect the city's uneven density field. The same ecological distinction between inter-specific (between species) and intra-specific (within species) competition also maps neatly to markets: rivalry between types (e.g., chains, operators, formats) versus crowding within a type (cannibalisation among a chain's own units).

Building on these insights, we propose a spatial HHI that is explicitly density-aware. In our construction, population is assigned to the nearest unit using Voronoi cells (with an optional gravity/Huff variant), producing unit-level shares that sum to one over the city (Huff, 1963; Okabe et al., 2000). Aggregating unit shares delivers type-level shares (e.g., by chain or operator). From these, we compute concentration at two layers: a unit-level spatial HHI that captures fragmentation across individual units and a type-level spatial HHI that captures dominance across types. Because these two views can point in different directions, many small units can still belong to a dominant type, we introduce a nested measure that separates inter-type dominance from intra-type crowding. This nested index preserves interpretability: high inter-type values flag cases where one type dominates its rivals, while the gap between type-level and outlet-level concentration flags internal fragmentation and potential self-cannibalisation within a type.

We build a density-aware spatial HHI by computing unit shares from Voronoi-assigned population (nearest-facility baseline, optional gravity/Huff), and study its behaviour in controlled simulations that vary siting (regular vs. random) and demand (uniform vs. clustered). We then extend the measure to a nested index that separates inter-type dominance from intra-type crowding, and operationalise siting as a tractable optimisation problem solved with a greedy-plus-swap heuristic. Finally, we demonstrate the approach on Warsaw case studies—Żabka, Biedronka vs. Lidl, and public primary schools - using open population grids and OSM facilities, and, where relevant, network distances (Aurenhammer, 1991; Huff, 1963; Church & ReVelle, 1974; Hakimi, 1964; Haklay & Weber, 2008; Boeing, 2017).

We position sHHI within recent work on geospatial decision-support: Voronoi-based map segmentation for trade-area delineation (Lee & Torpelund-Bruin, 2012; Lee, Torpelund-Bruin, & Lee, 2012), spatial interdependence in customer modelling (Baecke & Van den Poel, 2012), and network-aware spatial pattern mining (Yu, 2016). Our contribution differs by combining Voronoi cells with density weights and by separating inter-type rivalry from intra-type cannibalisation.

To support transparency and reuse, the properties of the spatial HHI (sHHI) can be explored via an online Shiny application (https://microeconomics.shinyapps.io/sHHI/). All estimation scripts and input data are openly available on GitHub (https://github.com/Endote/spatial-HHI/tree/master), providing open, reproducible geocomputation workflows in R/sf that are readily adaptable for policy scenarios.

1. From Aspatial Indices to Spatial Ecology: Toward a Density-Based Competition Metric

The empirical study of competition has long relied on a triad of indicator families that, while conceptually distinct, share a common aspatial foundation. Structural measures headed by the Herfindahl–Hirschman Index (HHI) and concentration ratios (C5, C10)—distil market power into aggregates of firm shares and remain central to debates on concentration and competition policy (Davies, 2021). Behavioural measures rooted in price-cost margins most famously the Lerner Index translate the price-marginal-cost gap into an elasticity-based indicator of monopoly power (Shaffer & Spierdijk, 2020). A third, hybrid class embeds cost-margin information in aggregated concentration frameworks, linking mark-ups with market shares under standard input and demand conditions. These indicators are serviceable in antitrust and industry studies, yet their use is often sector-dependent: HHI is routine in telecommunications and airlines with high fixed costs and entry barriers, C5/C10 are common in fast-moving consumer goods, and Lerner-style metrics are applied in regulated sectors such as pharmaceuticals and banking (Soldatos, 2021). Still, all three families implicitly treat space as frictionless: firms are presumed to exert identical pressure on one another regardless of distance or the density that ties consumers to place.

The spatial blind spot is striking given the long tradition of location theory. From Hotelling's linear city (Hotelling, 1929), through Salop's circular variant (Salop, 1979) and related spatial models (d'Aspremont et al., 1979), to contemporary spatial econometric and semiparametric competition games, theorists routinely embed distance, transport costs and neighbourhood effects in strategic interaction. Recent work extends these insights with agent-based models and spatial simulations of retail location, path dependence, and spatial competition (Miura & Shiroishi, 2019; Zhang & Robinson, 2022). Yet the resulting metrics seldom migrate into practice. Regulators still clear mergers on national-level HHIs; retail chains choose sites with heuristics rather than transparent peer-pressure indices; and urban planners lack benchmarks to judge whether the mix of pharmacies, emergency wards or secondary schools in a district is socially optimal. As the accessibility literature has shown, conventional measures often overlook the spatial heterogeneity of access conditions in dense urban settings, creating demand for geographically sensitive indicators (Chen & Chang, 2015).

Understanding spatial competition at granular scales is increasingly important. Spatial interactions between consumers and firms, and the spatial stability of urban submarkets, shape location decisions and effective market power (Kopczewska, 2020; Kopczewska & Ćwiakowski, 2021). In urban planning, fine-grained analyses inform zoning, infrastructure and service provision, helping address spatial inequalities in access (Batty, 2013; Neutens et al., 2012). Crucially, the growing availability of fine-grained geospatial data-address-level points of interest, raster-based population grids and open road/building layers-enables density-sensitive competition metrics and spatial disaggregation beyond administrative containers. With advances in data science and geostatistics, analysts can now assign market power and competitive interaction to explicit territories and simulate their dynamics, expanding both resolution and policy relevance (van Leeuwen & Lijesen, 2012). This matters for three constituencies. Firms in saturated cities must balance cannibalisation against coverage; without a spatial index, location decisions rely on intuition or black-box models. Regulators face local monopolies that slip beneath national thresholds; a density-aware measure would reveal pockets of excessive power invisible to conventional HHIs. Public authorities require diagnostics that capture how population density and facility proximity jointly determine access. Early applications e.g., Voronoi-based, population-weighted market shares for supermarkets demonstrate feasibility and policy relevance, showing how outlets in dense districts exert disproportionate influence and how spatially weighted concentration can diverge sharply from its non-spatial counterpart (Turolla, 2016).

Ecology offers both conceptual legitimacy and methodological guidance. Spatial competition has long been routine in ecology, where researchers map how plants compete for light or predators for territory. The workhorse is the Voronoi (Dirichlet) tessellation, which partitions space into mutually exclusive zones of influence: each location is assigned to its nearest seed (Aurenhammer, 1991). This geometry translates physical spacing into quantitative measures of neighbourhood interaction and crowding (Pielou, 1959; Pacala & Silander, 1985). Its simplicity has propelled it beyond ecology: network-Voronoi cells speed up k-nearest-neighbour queries (Kolahdouzan & Shahabi, 2004), Voronoi masks guide image segmentation

(Cheddad et al., 2008), and tessellation-based perturbations support modern machine learning pipelines (Zhong et al., 2020). The ecological precedent thus motivates a spatial competition index for firms: like organisms vying for resources, retailers and service providers vie for purchasing power embedded in residential density. A Voronoi-based approach allocates each consumer to the nearest facility and weights territorial claims by demographic mass, transforming qualitative insights of location theory into a quantitative analogue of territoriality.

Although scholars have proposed Voronoi- or Delaunay-based zones of influence and spatial concentration measures, innovations remain fragmented and case-specific. For instance, Delaunay-derived metrics in Queensland supermarkets reveal heterogeneous geographic competition across chains (Beare & Szakiel, 2009), while spatial diversion ratios and localised concentration indices can outperform national HHIs in retail mergers (Ellickson et al., 2020). GIS/AHP-based studies further show the value of spatial decision tools for retail site selection (Roig-Tierno et al., 2013). By fusing ecological theory (Tilman, 1988) with spatial econometrics, a unified, density-based spatial competition index can supply urban economists, planners and strategists with a demographically grounded indicator that supports store siting, antitrust scrutiny and equitable service provision (Birkin et al., 2002; Apparicio et al., 2008).

Finally, the ecological distinction between inter-specific and intra-specific competition provides a direct template for markets. Inter-specific (between-species) rivalry maps to inter-type competition (e.g., between chains, operators or formats), while intra-specific (within-species) rivalry maps to intra-type crowding—i.e., cannibalisation among a single chain's units. Any spatial index that respects territories and density should therefore separate these layers: diagnosing where a type dominates outsiders (inter-type) versus where its own demand is fragmented across many same-type units (intra-type). Embedding this separation in a single, interpretable framework is the key step from ecological inspiration to an operational tool for competition analysis.

2. New Indicator - spatially weighted HHI: Construction and Behaviour;

2.1 Derivations (From HHI to Voronoi-Assigned Shares)

This section brings together two ideas. The first is the classical Herfindahl–Hirschman Index (HHI), which summarises market structure from a set of shares. The second is the Voronoi (Dirichlet) tessellation, which turns locations of units into transparent "zones of influence." By computing each unit's share from the population assigned to its Voronoi zone, we obtain a spatial counterpart of HHI that reflects where people live and which unit is closest.

Let s_i denote the share of unit i and let shares sum to one. The (aspatial) HHI is

$$\mathrm{HHI} = \sum_i s_i^2.$$

If all n units have equal shares, $s_i = 1/n$ and $\mathrm{HHI} = 1/n$ (minimum). If a single unit captures everything, $\mathrm{HHI} = 1$ (maximum). Intuitively, HHI increases when a few units hold most of the mass and decreases when mass is evenly spread.

Voronoi diagrams partition space into cells nearest to each unit, offering a canonical geometric structure (Aurenhammer, 1991). Every point inside a polygon is closer to its generating unit than to any other. A Voronoi tessellation is constructed by placing a finite set of generator points on a plane and drawing the perpendicular bisectors of every pairwise segment; the resulting network of edges delineates cells that exhaustively cover the plane without overlap. Because the algorithm depends only on distance, it generalises naturally from ecology to data science, where proximity is the bedrock of clustering, classification and image analysis. Figure 1 visualises a canonical two-dimensional tessellation: fifteen randomly placed units generate mutually exclusive cells whose boundaries trace the locations of equidistance. In an economic context, these seeds could be retail outlets, and the polygon areas are the catchments over which they exert first-mover access to customers. Our catchments rely on generalised Voronoi polygons, a standard tool for geospatial segmentation (see Lee & Torpelund-Bruin, 2012; Lee et al., 2012).

Figure 1. Voronoi Tessellation of Random Seed Points

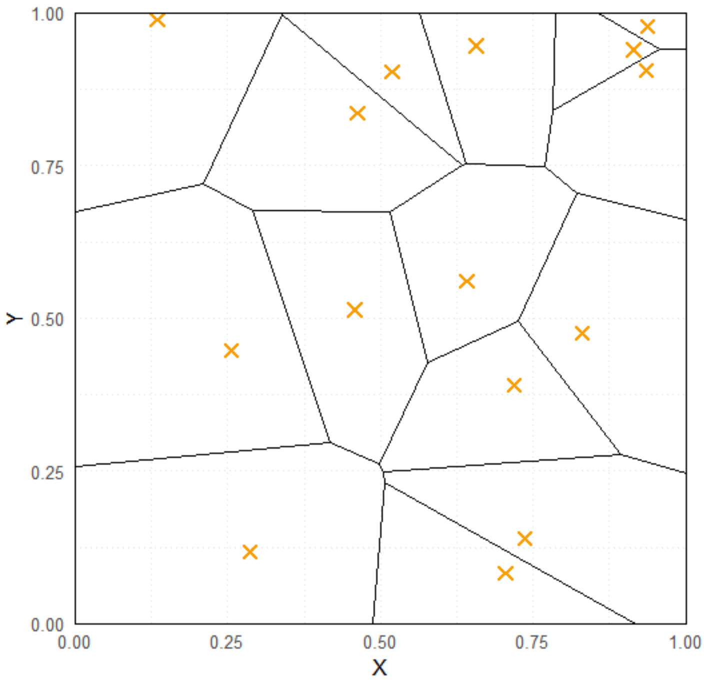

Source: own elaboration.

Voronoi tessellation and proportional population assignment

Let $\{m_i\}$ denote the set of centroids. Compute Voronoi polygons $\{V_i\}$ from $\{m_i\}$ and clip them to the city boundary B so polygons do not extend beyond the study area. Population comes from a regular grid of census cells $\{C_j\}$ with known counts P_j.

Each census cell contributes proportionally to the polygons it intersects:

$$P_{ij} \;=\; P_j \times \frac{\mathrm{Area}(C_j \cap V_i)}{\mathrm{Area}(C_j)}.$$

The total population in Voronoi polygon V_i is

$$P_i \;=\; \sum_j P_{ij}.$$

This proportional rule is robust to grid resolution: if a census cell straddles two polygons, its count is split by area, not lost or double-counted.

Spatially weighted shares for units

The simplest spatial share for unit i uses the polygon totals:

$$q_i \;=\; \frac{P_i}{\sum_k P_k}.$$

In contrast to prior segmentation work focused on boundary detection (e.g., Lee & Torpelund-Bruin, 2012; Lee et al., 2012), we attach population-density weights to cells to obtain share-comparable exposure surfaces.

Because people concentrate in some polygons and are sparse in others, we also account for how tightly population is packed in each polygon. Define the polygon's average density

$$p_i \;=\; \frac{P_i}{A_i},$$

where $A_i = \text{Area}(V_i)$. There are two equivalent and transparent ways to combine "how many people" (P_i) with "how dense" (p_i) into one share per unit.

Variant A (combine normalised components, then renormalise once). Form the normalised population share $q_i = P_i/\sum_k P_k$ and the normalised density weight $r_i = p_i/\sum_k p_k$. Combine them multiplicatively and renormalise to get valid shares:

$$s_i \;=\; \frac{q_i\, r_i}{\sum_\ell q_\ell\, r_\ell}.$$

This keeps interpretation clear—q_i says "how many", r_i says "how dense"—and avoids overweighting either term.

Variant B (single score, then normalise). Compute an unnormalised score

$S_{i'} \;=\; P_i \times p_i \quad \left(\text{or, more generally } S_{i'} = P_i^{\,\gamma}\, p_i^{\,\delta}\right)$,and set the share $s_i = S_{i'}/\sum_k S_{k'}$. Choosing γ and δ lets the analyst tune the emphasis on "how many" vs "how dense" (the paper's baseline sets $\gamma = \delta = 1$). This one-step normalisation avoids double-compounding intermediate ratios.

Either way, the s_i sum to one across units and directly reflect distance (who is nearest) and density (where people cluster).

Spatial HHI at the unit level

With spatial shares s_i in hand, the spatial HHI (units) is computed exactly like the classical index:

$$s\text{HHI}_{\text{units}} \;=\; \sum_i s_i^2.$$

Interpretation remains familiar. If every unit serves a similar population under the nearest-unit rule, $\text{sHHI}_{\text{units}}$ is low. If a few units capture most of the Voronoi-assigned population - typically because they sit amid dense neighbourhoods - $\text{sHHI}_{\text{units}}$ is high. The difference from the classical HHI is not the formula, but the spatially grounded shares that enter it.

2.2 Simulation of behaviour - synthetic screening (2 - 4 - 8 points of sale);

To examine how the spatial HHI (units) reacts to spatial and demographic heterogeneity, we run a simple computational experiment on a stylised city (a unit square). Two dimensions are varied: where units are placed and how people are distributed. For locations, we consider a regular arrangement (evenly spaced units) and a random arrangement (independent draws). For population, we use a uniform field and a random field with pockets of higher and lower density. For each scenario we evaluate three market sizes, with $n = 2,4,8$ units. In every run we (i) construct Voronoi polygons from the unit locations, (ii) assign census-grid population to polygons proportionally by area of overlap, (iii) compute each polygon's population P_i and average density $p_i = P_i/A_i$, (iv) convert these into spatial shares s_i (baseline Variant B: score $S_{i'} = P_i\, p_i$, then $s_i = S_{i'}/\sum_k S_{k'}$), and (v) calculate $\mathrm{sHHI_{units}} = \sum_i s_i^2$. Repeating the procedure across scenarios reveals how geometry and density shape concentration.

Figure 2. Behaviour of the Spatial HHI (units) under alternative location–population scenarios

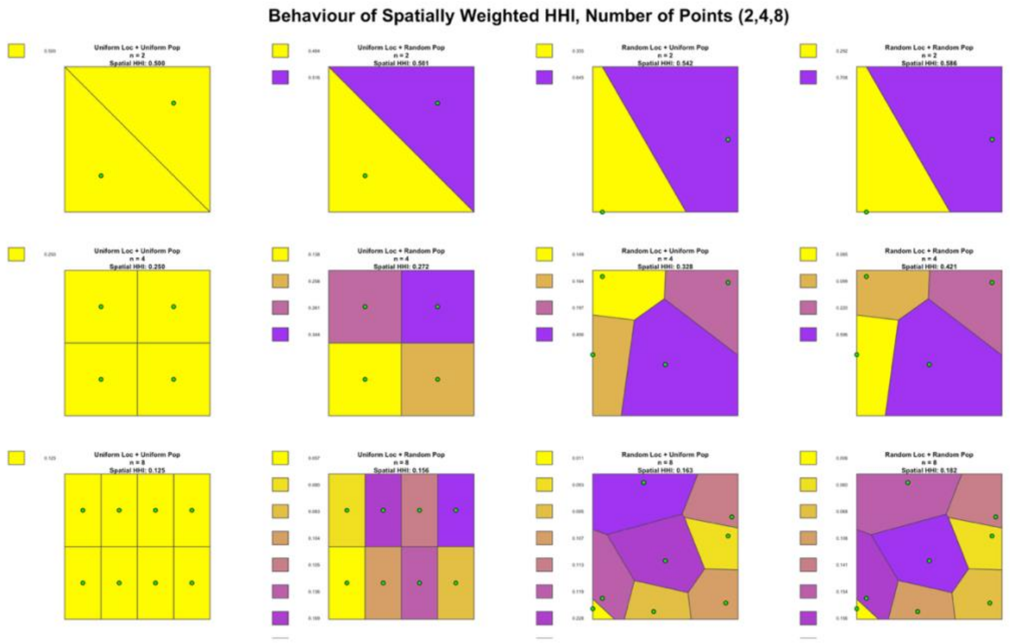

Rows: market size n={2,4,8} firms. Columns: four scenarios : (1) Regular firms' locations + Uniform population; (2) Regular firms' locations + Random population; (3) Random firms' locations + Uniform population; (4) Random firms' locations + Random population. Own elaboration.

Source: own elaboration.

Figure 2 (panel grid) shows representative outcomes that match the broader Monte-Carlo pattern. With regular locations and uniform population, shares are equal and the spatial HHI attains its theoretical minimum $1/n$: 0.500 for two units, 0.250 for four, and 0.125 for eight. Holding locations regular but making population random introduces demand pockets; units covering denser quadrants gain share and concentration ticks up (e.g., $n = 4$: 0.272). Holding population uniform but making locations random produces irregular catchments; unequal polygon areas lift concentration further (e.g., $n = 4$: 0.328). When both forces act together—random locations and random population—effects compound and the spatial HHI is highest (e.g., $n = 2$: 0.586; $n = 4$: 0.421; $n = 8$: 0.182).

Three regularities emerge. First, either uneven siting or clustered demand is sufficient to raise concentration above the equal-share benchmark; combining them amplifies the effect. Second, increasing the number of units lowers the index in every scenario: with more generators, Voronoi cells become smaller and the scope for any one unit to dominate shrinks. Third, the ranking of scenarios is stable across draws: regular-uniform is always lowest; random-random is always highest, with the mixed cases in between. This is exactly the comparative statics one would expect from a distance-based assignment over a heterogeneous density field, and it validates the diagnostic power of the spatial HHI: the index moves in a predictable, interpretable way when the geometry of catchments or the distribution of people becomes more uneven.

Economically, the patterns are intuitive. Under uniform population, concentration rises mainly because catchments become unequal - an immediate consequence of random unit placement. Under regular placement, concentration rises because demand mass is no longer evenly split - units that happen to cover high-density patches gain share. Where both occur, the same unit can enjoy a double advantage (a large cell sitting on a dense patch), and the spatial HHI reflects that compounding. For planners and managers, the implication is direct: to reduce concentration, add capacity in underserved dense pockets (shrinking both cell size and density imbalance); to grow a focal unit's share without excessive cannibalisation, target dense areas where rival catchments are large but internally weak.

2.3 Optimisation: siting under intra-type competition

In the framework, all units belong to a single type. This setting captures cases such as convenience stores of the same type or a single retail chain's stores or public primary schools (one municipal provider). Here, the only relevant rivalry is within-type (intra-type) competition: each new unit reduces the catchments of its peers but does not compete with another type. The objective is therefore to adjust the placement of an additional unit so as to improve intra-type equity. For a retail chain, this means reducing cannibalisation between stores while preserving coverage. For a planner managing schools, this means reducing overload in large catchments and shortening trips for underserved pupils. Formally, the measure of interest is the unit-level spatial HHI:

$$s\text{HHI}_{\text{units}} = \sum_j s_j^2,$$

where s_j is the spatial share of unit j, defined by Voronoi-assigned, density-weighted population.

Adding a new unit y creates a new Voronoi cell and redistributes mass from existing cells, which changes the set $\{s_j\}$. The optimisation problem is thus: For a manager (retail chain): Choose y that minimises the new unit-level sHHI, i.e.

$$y^{\star} = \underset{y \in Y}{\operatorname{argmin}}\ \text{sHHI}_{\text{units}}(X \cup \{y\})$$

For a planner (public schools): Choose y that minimises inequality of access, proxied by the same sHHI across schools:

$$y^{\star} = \underset{y \in Y}{\operatorname{argmin}}\ \mathrm{sHHI}_{\mathrm{units}}(X \cup \{y\}).$$

In both cases, the function is identical; the interpretation differs. The procedure is therefore a single-type special case of the general optimisation in Section 3. Detailed derivations and pseudocode are provided in Appendix A.

3. Extension: Competition Between and Within Types: A Nested Density-Based Index of Spatial Competition

3.1 Methodology description

Retail rivalry unfolds simultaneously between chains or formats (inter-type competition) and within the same chain or format (unit intra-type crowding). Classic spatial models explain why both layers matter: firms differentiate by location (Hotelling, 1929), consumers face distance frictions and probabilistic choice (Reilly, 1931; Huff, 1963), and catchments partition urban space in ways naturally represented by Voronoi tessellations (Okabe et al., 2000). Concentration itself is typically measured by the Herfindahl–Hirschman Index (HHI), widely used in antitrust practice (Rhoades, 1993; U.S. Department of Justice & Federal Trade Commission, 2023). Yet a single, population-aware statistic that nests inter- and intra-type competition and respects overlapping catchments has been missing. The objective of the NSCI is therefore to keep the spatial HHI logic while defining shares from density-weighted, spatially assigned population.

Let G denote the set of population grid cells, J the set of outlets or facilities, and T the set of types, where a type may represent a chain, operator, ownership group or service format. Each grid cell $g \in G$ has population P_g. The cell-level weighted demand used throughout the index is P_g^{η}, where $\eta > 0$ is the density-weighting parameter. The baseline case is $\eta = 1$, which gives pure population weighting. Values $\eta > 1$ place extra emphasis on dense/high-population cells, while $0 < \eta < 1$ compresses differences between cells. Total weighted demand is:

$$W_{\eta} = \sum_{g \in G} P_g^{\eta}.$$

Let a_{gj} be the assignment weight from cell g to outlet j. Under the nearest-facility Voronoi rule, $a_{gj} = 1$ for the outlet receiving cell g and $a_{gj} = 0$ otherwise. Under an area-intersection implementation, a_{gj} is the fraction of grid-cell area assigned to outlet j. Under a Huff/gravity rule, a_{gj} is a fractional choice probability decreasing with distance. In all cases:

$$a_{gj} \in [0,1], \qquad \sum_{j \in J} a_{gj} = 1.$$

The weighted demand assigned to outlet j is:

$$Q_j^{(\eta)} = \sum_{g \in G} a_{gj} \, P_g^{\eta},$$

and the outlet-level spatial share is:

$$s_j = \frac{Q_j^{(\eta)}}{W_\eta}.$$

Because assignment weights sum to one within each grid cell, the outlet shares also sum to one:

$$\sum_{j \in J} s_j = 1.$$

Let $J_t \subset J$ denote the set of outlets belonging to type t. The type-level spatial share is obtained by aggregating outlet shares within each type:

$$S_t = \sum_{j \in J_t} s_j.$$

The inter-type, or type-level, spatial HHI is:

$$H_{\text{inter}} = \sum_{t \in T} S_t^2.$$

This term measures concentration between chains, operators or service formats. It is high when one type controls a large share of spatially assigned demand and low when demand is spread more evenly across types.

Within each type, internal concentration is measured by:

$$I_t = \sum_{j \in J_t} \left(\frac{s_j}{S_t}\right)^2, \qquad S_t > 0.$$

The statistic I_t describes how evenly type t's own spatial demand is distributed across its outlets. If I_t is close to 1, one outlet dominates most of the type's assigned demand. If I_t is close to $1/|J_t|$, the type's demand is distributed almost evenly across its outlets. Thus, I_t is an internal load-allocation measure. It should not be interpreted as observed sales diversion by itself.

The outlet-level spatial HHI is:

$$H_{\text{outlet}} = \sum_{j \in J} s_j^2.$$

Using the within-type definition above, the same quantity can be written as:

$$H_{\text{outlet}} = \sum_{t \in T} S_t^2 \, I_t.$$

This identity is central: it shows that the outlet-level index is the sum of within-type concentration terms weighted by squared type shares, not by simple type shares. The squared weight is necessary for the endpoint interpretation of the nested index to be mathematically correct.

The Nested Spatial Competition Index is then defined as:

$$NSCI_{\alpha} = \alpha H_{\text{inter}} + (1-\alpha) H_{\text{outlet}}, \qquad \alpha \in [0,1].$$

Equivalently:

$$NSCI_{\alpha} = \alpha \sum_{t \in T} S_t^2 + (1-\alpha) \sum_{t \in T} S_t^2 \, I_t.$$

The parameter α is the inter/outlet mixing weight. If $\alpha = 1$, the index collapses to the type-level spatial HHI. If $\alpha = 0$, it collapses to the outlet-level spatial HHI. Intermediate values implement a transparent trade-off between external market power across types and fragmentation across individual outlets.

The difference between the two concentration layers is also informative:

$$\Delta_{\text{frag}} = H_{\text{inter}} - H_{\text{outlet}} = \sum_{t \in T} S_t^2 \, (1 - I_t).$$

Equivalently:

$$\Delta_{\text{frag}} = 2 \sum_{t \in T} \sum_{\substack{j<k \\ j,k \in J_t}} s_j \, s_k.$$

This gap measures how much type-level dominance is internally fragmented across multiple outlets of the same type. In a retail chain interpretation it is a proxy for potential self-cannibalisation or internal network crowding, but it is not a direct behavioural estimate of sales diversion. Direct self-cannibalisation is evaluated in the siting problem through the own-type mass reallocated to a candidate site.

Methodologically, the index combines distance-based assignment (Voronoi or Huff), density-weighted demand P_g^{η}, and HHI's quadratic aggregation into a single economic diagnostic. It remains label-invariant and bounded in $[0,1]$. Cross city comparisons are meaningful when the grid resolution, type definitions, distance metric and assignment rule are held constant.

3.2 Simulation of behaviour - synthetic screening (3 chains: 4–2–3 points of sale)

The synthetic experiment illustrates how the decomposition behaves when outlet-level and type-level concentration point in different directions. We simulate three chains with asymmetric footprints: chain A has four outlets, chain B has two, and chain C has three. Outlets are placed in the unit square and the demand field is uniform, so differences in shares arise from spatial geometry rather than exogenous demand clusters. Voronoi catchments are intersected with the grid to compute outlet shares s_j, then aggregated into type shares S_t, within-type concentration values I_t, H_{outlet}, H_{inter}, and $NSCI_\alpha$.

Figure 3. Inter- vs. intra-network competition in a synthetic screening (A=4 units, B=2, C=3)

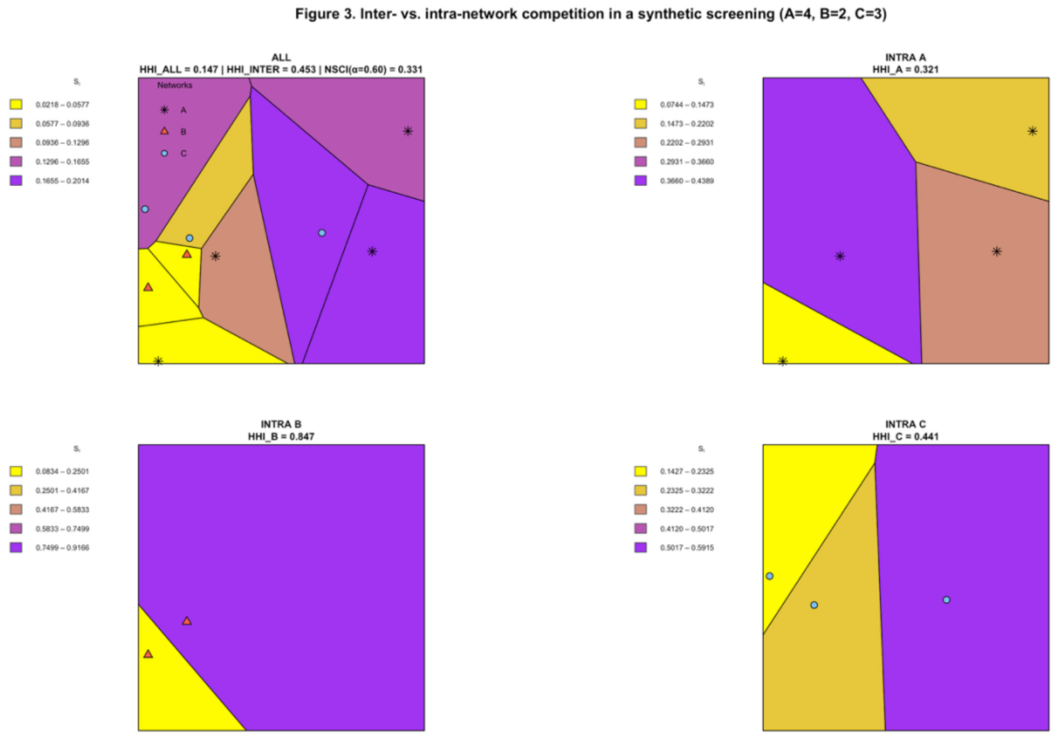

Description: Panel layout. Top-left (ALL): Voronoi catchments for all 9 units on a uniform demand field. Colours show each outlet share s_j; symbols denote networks (A = ★, B = △, C = ○). Reported indices: H_outlet = 0.147, H_inter = 0.453, and NSCI_α with α = 0.60 equals 0.331. Top-right and bottom row (INTRA A/B/C): Voronoi maps restricted to each network's own outlets, reporting within-type concentration I_t. Higher I_t means a more uneven internal allocation of that type's demand; lower I_t means a more evenly fragmented internal network. Interactive simulation: available online in the Shiny app.

Source: own elaboration.

The figure reports $H_{\text{outlet}} = 0.147$, $H_{\text{inter}} = 0.453$, and $NSCI_{0.60} = 0.331$. The NSCI arithmetic follows directly from the convex combination:

$$NSCI_{0.60} = 0.60 \cdot 0.453 + 0.40 \cdot 0.147 = 0.331.$$

Changing α changes the economic lens without changing the underlying shares. With $\alpha = 0.8$, the index moves closer to the type-level antitrust perspective:

$$NSCI_{0.80} = 0.80 \cdot 0.453 + 0.20 \cdot 0.147 = 0.392.$$

With $\alpha = 0.3$, the index places more emphasis on outlet-level fragmentation:

$$NSCI_{0.30} = 0.30 \cdot 0.453 + 0.70 \cdot 0.147 = 0.239.$$

The within-type maps report $I_A = 0.321$, $I_B = 0.847$, and $I_C = 0.441$. Chain B therefore has the most internally concentrated network: one of its two outlets dominates most of B's assigned demand. Chain A is the most internally dispersed because four outlets divide its demand more evenly. Chain C lies between the two. These values should be read as internal allocation statistics, not as direct cannibalisation estimates. Potential self-cannibalisation is instead reflected by the fragmentation gap $H_{\text{inter}} - H_{\text{outlet}}$ and, in the optimisation problem, by the own-type demand mass reallocated to a candidate site.

Economically, the example shows why the nested structure is useful. A market can have a relatively low outlet-level concentration because demand is split across many individual facilities, while still having a high type-level concentration because many of those facilities belong to the same chain or format. The NSCI keeps both views visible. It therefore avoids the false comfort of saying that a market is competitive merely because many outlets exist, and it avoids the opposite mistake of treating every dense network as equally harmful without checking how its internal demand is distributed.

3.3 Optimisation: choosing the best location with inter- and intra-type competition

The siting problem uses the same objects as the index. Let X denote the current set of outlets, partitioned into types T, and let $\mathcal{Y}$ denote feasible candidate sites. Adding a candidate site changes the assignment weights a_{gj}, hence the outlet shares s_j, type shares S_t, within-type concentration terms I_t, and the resulting index values. The optimisation differs depending on the decision-maker.

A planner minimises the system-wide nested concentration index. For m new sites, the planner's problem is:

$$Y^{\star}_{\text{planner}} = \arg\min_{Y^{\star} \subseteq \mathcal{Y},\, |Y^{\star}|=m} NSCI_{\alpha}(X \cup Y^{\star}),$$

where:

$$NSCI_{\alpha}(X \cup Y^{\star}) = \alpha \sum_{t \in T} (S_t')^2 + (1-\alpha) \sum_{t \in T} (S_t')^2 \, I_t'.$$

Primes denote values after adding the candidate set. For public services, this objective has a direct access-equity interpretation: lower outlet-level concentration means demand is more evenly distributed across facilities. When only one type exists, $H_{\text{inter}} = 1$ is constant, so minimising $NSCI_{\alpha}$ is equivalent to minimising H_{outlet}.

A manager of a focal type τ faces a different economic problem. The manager does not generally want to minimise city-wide concentration. The manager wants to capture demand from rival types while avoiding excessive reallocation from its own existing outlets. For a single candidate site y, define the set of cells that would switch to the candidate under nearest-facility assignment:

$$W_{\text{win}}(y) = \{g \in G : d(g, y) < d(g, x_{j(g)})\},$$

where $j(g)$ is the unit currently serving cell g. The weighted demand captured from rival types is:

$$A_{\tau}(y) = \sum_{\substack{g \in W_{\text{win}}(y) \\ type(j(g)) \neq \tau}} P_g^{\eta},$$

and the weighted demand taken from the focal type's own outlets is:

$$B_\tau(y) = \sum_{\substack{g \in W_{\text{win}}(y) \\ type(j(g))=\tau}} P_g^{\eta}.$$

The candidate's managerial score is:

$$M_\kappa(\tau; y) = \frac{A_\tau(y)}{W_\eta} - \kappa \frac{B_\tau(y)}{W_\eta}, \qquad \kappa \in [0,1].$$

The parameter κ is the self-cannibalisation penalty. If $\kappa = 0$, the manager cares only about demand won from rivals. If $\kappa = 1$, own-type demand reallocated from existing outlets is treated as fully costly. Intermediate values allow the analyst to represent partial tolerance for internal reallocation.

For multiple additions, an exact search over all candidate subsets is combinatorial. The thesis therefore uses a greedy-plus-swap heuristic. At each step, the algorithm evaluates candidate sites with the same density-weighted assignment used in the index. For the planner objective it selects the site that gives the lowest updated $NSCI_\alpha$. For the manager objective it selects the site with the highest $M_\kappa(\tau; y)$. A local swap phase then tests whether replacing one selected site with a nearby feasible candidate improves the relevant objective. This keeps measurement and decision support aligned: the same spatial shares that define concentration also drive the location recommendation.

The economic interpretation is straightforward. A site is attractive for a manager when it captures a large rival mass $A_\tau(y)$ in a dense pocket while keeping own-type reallocation $B_\tau(y)$ small. A site is attractive for a planner when it reduces system-wide concentration by lowering type-level dominance, outlet-level concentration, or both. The two objectives use the same spatial data structure but answer different questions: private expansion strategy versus public or regulatory spatial balance.

4. Case Studies: Proof of Concept

4.1 Study Area and Data Acquisition

We focus on Warsaw, the capital and largest city of Poland. As of June 2025, it had about 1.864 million residents, spans 517.2 km², and an average population density of ≈3,600 people/km²—very high by Polish standards, but moderate among European capitals (roughly Berlin-like, below London/Madrid, far below Paris/Barcelona). The urban fabric combines a dense pre-war core and post-war housing estates, with strong radial corridors and the Vistula acting as a natural barrier bridged at discrete points. Note that the citywide average masks sharp internal contrasts: central districts frequently exceed 8–12k people/km², while outer areas fall to 1–3k/km². Retail and public services are correspondingly polycentric - high facility intensity in inner districts, sparser coverage toward the periphery. This heterogeneity makes Warsaw a natural testbed for a density-aware spatial index. For descriptive context we report the latest official city headcount, whereas the spatial weighting used in the case studies is based on the latest openly available nationwide census grid, NSP 2021 provided by Polish Central Statistical Office.

We showcase three contrasting settings that together span the main use-cases of the Spatial HHI. Żabka represents a monopoly-like format with ultra-dense siting, highlighting intra-type (within-network) crowding and cannibalisation. Biedronka vs. Lidl provides a citywide duopoly, where many outlets coexist but rivalry is primarily inter-type (between networks) and spatially asymmetric. Public primary schools offer a non-market counterpoint in which the objective is equitable access, not profit-useful for showing how the same density-aware machinery guides planner-oriented siting on the urban fringe. Together, the trio tests the index across private and public services, low vs. high outlet density, and cannibalisation vs. rivalry-precisely the dimensions the method is designed to separate and diagnose.

Data sources and integration

We combine three complementary spatial layers to build the inputs required by the Spatial HHI pipeline:

1. Administrative boundary (shapefile). We use the official city boundary to clip all geometry and keep computations within Warsaw. All datasets are re-projected to a metric CRS (for distances/areas), and a light spatial buffer is applied before tessellation to avoid edge artefacts along the boundary and the Vistula.

2. Population grid (raster/grid). We use the NSP 2021, latest available, census grid to provide fine-grained counts for spatial weighting. Population from each grid cell is assigned to Voronoi polygons proportionally to the area of overlap, so cells that straddle polygon borders are split rather than lost or double-counted. Zero-population cells are retained to preserve geometry but do not influence shares.

3. Point features (POIs). Retail: brand-filtered OpenStreetMap points/polygons for Żabka (Polish small convenience store), Biedronka, Lidl (using brand, name, shop=* tags; polygons converted to representative points). Public services: the municipal register of public primary schools (official school IDs, addresses). Attributes are harmonised (names, chains, IDs), and obviously closed/duplicate records are removed. Żabka requires special care because the same outlet can appear as multiple closely spaced POIs (e.g., point + building polygon).

Data cleaning: collapsing duplicates to a single representative point.

Spatial data sources often represent one real-world unit by several nearby points or polygons. To avoid multiple seeds for the same unit, we cluster by proximity and keep a single representative—the medoid. Let $X = \{x_1, \ldots, x_n\}$ be recorded unit points in metric coordinates. Fix a small distance threshold t (e.g., 30–50 m). Build an adjacency matrix

$$a_{ij} = \begin{cases} 1 & \text{if } 0 < d(x_i, x_j) < t, \\ 0 & \text{otherwise,} \end{cases}$$

where $d(\cdot,\cdot)$ is Euclidean distance. Treat $A = [a_{ij}]$ as an undirected graph $G(V, E)$ and find its connected components (clusters). For each cluster $C \subset V$, choose the medoid

$$m_C = \underset{x_j \in C}{\operatorname{argmin}} \sum_{x_i \in C} d\,(x_i, x_j),$$

i.e., the point whose total distance to other members of C is minimal. Using these medoids as seeds prevents one facility from generating several overlapping polygons.

Workflow integration.

After re-projection and de-duplication, we build Voronoi polygons from the medoids, clip them to the city boundary, and allocate census-grid population to polygons proportionally by intersection area. For each polygon we compute total population and area-based density, derive spatial shares for units (as defined in Section 2), and finally compute the spatial HHI for the case studies (Żabka; Biedronka vs. Lidl; primary schools).

All input data and reproducible code for cleaning, tessellation, assignment, index calculation, and optimisation are provided as supplementary online materials (Data S1–S3; Code S1).

4.2 Small franchise convenience stores - monopoly-like network (intra-type crowding)

Żabka is a phenomenon in Poland's urban retail: a very small footprint convenience store (typical sales area around 50–70 m²) scaled into a vast, ultra-dense network. Units are sited at residential entrances and transit nodes, operate long hours (commonly ~06:00–23:00; selected formats 24/7), and via legal exemptions or owner-operated rules are often the only widely available branded option on non-trading Sundays. In practice this yields very short inter-store distances, near-ubiquity in inner districts, and numerous but small catchments that aggregate to format-level dominance in dense neighbourhoods. These traits map precisely to our framework: large spatial shares in high-density areas, low outlet-level fragmentation, and strong type-level concentration.

Figure 4 (left panel) (Voronoi catchments and spatial shares) shows that the catchments of all Żabka outlets tile almost the entire city. Most polygons are yellow, indicating very small per-outlet spatial shares (low customers-per-store density). Only a few purple hotspots appear—dense inner-city pockets where one outlet's catchment overlaps unusually high potential demand or where local spacing yields a slightly larger cell. In short: the network is ubiquitous, the typical catchment is tiny, and unused territory is scarce.

The outlet-level spatial HHI (within the Żabka type, across units) equals 0.0033 (Figure 4), which is extremely close to the equal-share benchmark for a network with several hundred outlets. Because only one type is present in this figure, the type-level (inter-type) spatial HHI is mechanically 1.0.

Is this "good" for the city? From a coverage perspective, the yellow sea means the network meets potential demand almost everywhere (short walks, long opening hours). From a competition perspective, however, such ubiquity implies near-zero inter-type pressure in the convenience niche: a marginal Żabka chiefly reallocates demand within the chain rather than taking it from rivals. For policy and planning, that distinction matters—robust format-level rivalry may be absent even when "many outlets" are visible on the street.

Figure 4. Żabka network in Warsaw

Figure 4. Zabka network in Warsaw

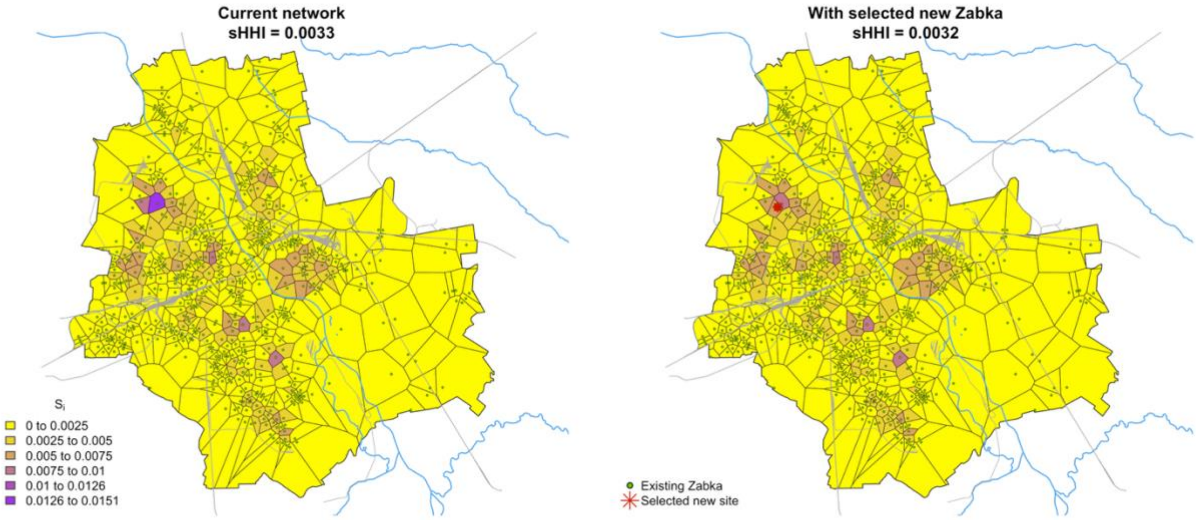

Description: Left panel: Voronoi catchments for all existing Żabka stores. Right panel: Result after placing the algorithmically selected site (red star) on the north-east fringe. Code and data: available on GitHub.

Source: own elaboration.

4.3 Mid-size supermarkets as a citywide duopoly (full-basket grocery)

In contrast to Żabka's ultra-dense micro-format, Biedronka and Lidl operate full-basket supermarkets with much larger floor areas, fewer but higher-capacity units, and longer inter-store distances. Their catchments are larger and frequently overlap across many districts, creating a head-to-head rivalry at the district scale. Coverage is asymmetric - Biedronka is more numerous, while Lidl is more selective in site choice - so citywide competition takes the form of a duopoly in which local dominance alternates between the two. Within our index this yields moderate outlet-level dispersion but a pronounced inter-type component, with neighbourhood pockets where one brand clearly leads and others where margins are thin.

Figure 5 contrasts three views of the same market. In the left panel (ALL), Voronoi catchments and spatial shares are computed for both chains jointly (red = Biedronka, blue = Lidl). Outlet-level concentration is very low (sHHI_ALL = 0.009) because shares are dispersed across 223 stores citywide, yet type-level concentration is high (sHHI_INTER = 0.712): despite many outlets, most spatial demand is captured by just two types, a classic duopoly. The map reveals broad overlap in central districts alongside district-scale pockets where one chain dominates the density field. The middle panel focuses on Biedronka (172 stores). Its within-type concentration is low (sHHI_B = 0.011), consistent with a large network whose total spatial share is split fairly evenly across many small catchments. The right panel isolates Lidl (51 stores). With fewer sites, catchments are larger and more uneven, yielding a higher within-type concentration (sHHI_L = 0.044). Together, these patterns describe an oligopolistic geometry: at the outlet level competition is intense, especially in the centre where catchments interlock, while at the type level rivalry is tight but asymmetric—Biedronka's footprint is broader and more uniform, Lidl's sparser and more selective—producing neighbourhoods where one brand clearly leads. The nested index (NSCI, $\alpha = 0.60$) reflects this split, with a sizeable inter-type component alongside chain-specific intra-type structures (Biedronka's higher cannibalisation risk versus Lidl's larger per-site pulls). From a planning perspective, reducing place-based dominance points to facilitating entry in single-brand pockets, especially where population is dense. From a managerial perspective, Lidl can grow share by targeting districts where Biedronka's catchments are large but internally weak, while Biedronka should avoid saturating already fine-grained cores and instead pursue underserved dense fringes or rival-led districts where inter-type gains exceed intra-type losses.

Figure 5. Biedronka vs. Lidl — spatial HHI and nested structure;

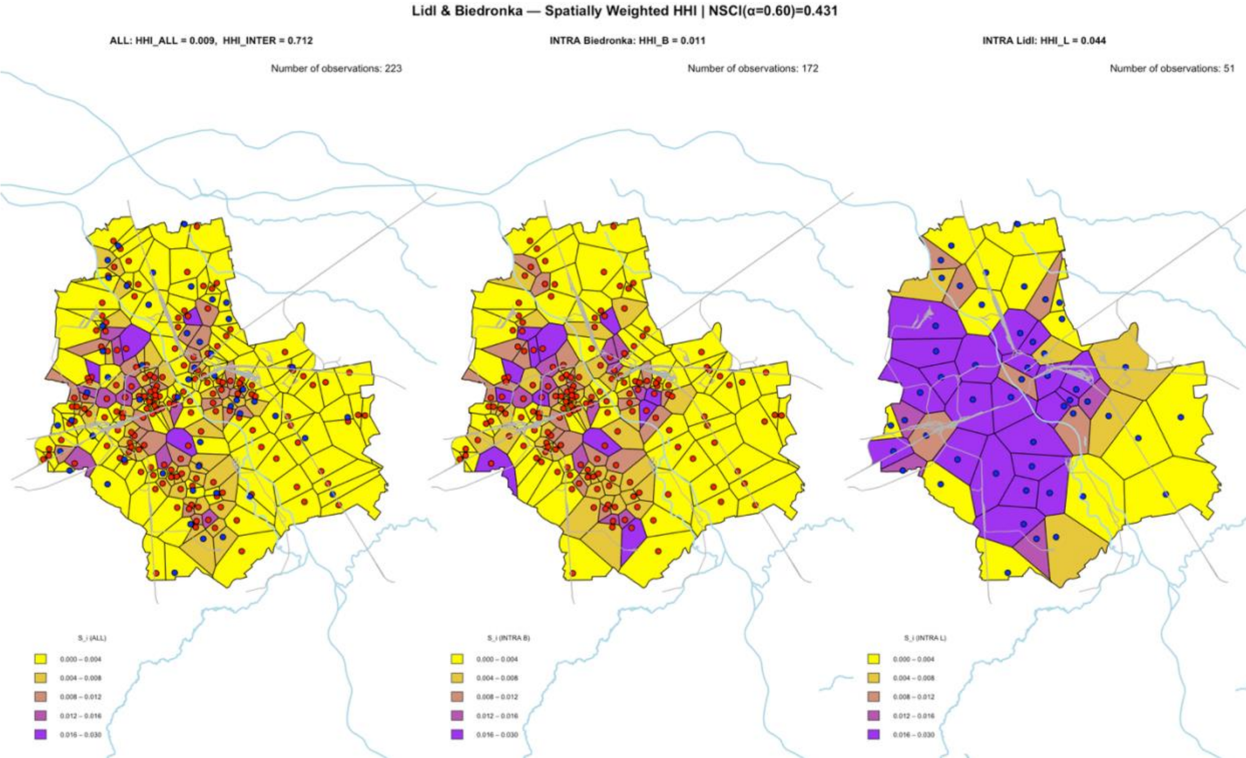

Description: Left panel: both chains together; middle panel: within-Biedronka spatial shares; right panel: within-Lidl spatial shares. Codes and data: available on GitHub

Source: own elaboration.

4.4 Primary schools as a public-service example

Primary schools are anchored in residential patterns and legally defined catchments, serving pupils roughly ages 6–15. In Warsaw, there are ~220 city-run primary schools, educating on the order of ~140,000 pupils, i.e. about ~640 pupils per school on average. This network is designed around proximity and equity rather than simple cost optimisation, with capacity and neighbourhood morphology shaping effective access. Rapid, partly uncoordinated suburban expansion has produced marked imbalances: peripheral schools in fast-growing housing estates tend to be very large and heavily loaded, while central schools - a legacy of denser, centrally planned provision -are more closely spaced yet often serve smaller cohorts in ageing, gentrifying districts. The consequence is uneven load and additional transport needs, as pupils from the urban fringe travel further to find available capacity.

In the baseline map (left, Figure 6), most school catchments are yellow (small per-school shares), but several brown/purple polygons appear on the urban fringe - new housing estates with no nearby schools and high concentrations of pupils aged 6–15. This is the classic footprint of uncoordinated suburban growth: the edge adds households faster than facilities, so peripheral schools inherit oversized catchments, while inner-city schools - a legacy of denser, centrally planned provision - sit closer together and serve smaller cohorts (Batty, 2013; Ewing & Hamidi, 2015). Adding one new school (right, red star) splits an overlarge, dense polygon and lowers the outlet-level Spatial HHI from 0.0180 to 0.0168. Unlike the retail cases, there is no inter-type rivalry here; the optimisation target is explicitly planner-oriented to decrease concentration / access inequality by trimming the largest and densest catchments. The gain is practical: shorter expected access distances for pupils in the newly served estate and reduced load pressure on adjacent schools. In a sprawling city, the greedy siting logic therefore prioritises edge districts where demand is heavy and coverage thin rather than the already well-served core (Neutens, Delafontaine, Scott, & De Maeyer, 2012).

The policy implication follows directly: more of the same in the centre yields little, whereas strategic additions at the fringe produce measurable equalisation of access and load. A programmatic rollout guided by the same density-aware index would systematically rebalance the network in step with residential growth.

Figure 6. Primary schools in Warsaw

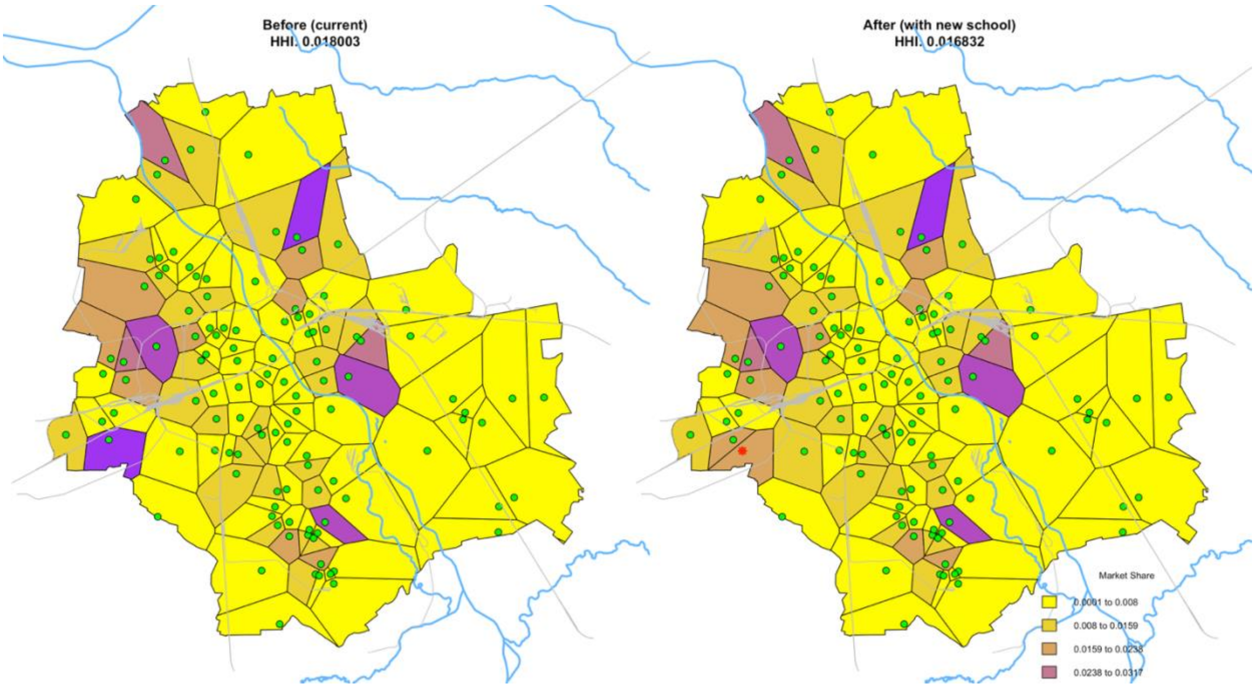

Description: Left panel: Voronoi catchments for existing public primary schools, coloured by

spatial share (pupils-per-school proxy). Right panel: Result after setting the algorithmically selected school (red star). Codes and data: available on GitHub.
Source: own elaboration.

Conclusions

This thesis builds and applies a density-aware spatial HHI that computes outlet (unit) shares from Voronoi-assigned population and aggregates them to type (network) shares. We separate rivalry into inter-type dominance and intra-type crowding, and we link the metric to a practical siting algorithm (greedy + local swaps) so the same index that diagnoses concentration also guides location choice (Church & ReVelle, 1974; Hakimi, 1964).

A strength of this spatial, density-aware approach is that its comparative statics are intuitive. Concentration rises when siting is uneven (units bunched into a corner) or when population is clustered (dense pockets), and it rises even more when both occur together. Conversely, adding a unit to an underserved dense pocket can materially reduce unit-level concentration without changing the citywide unit count. These patterns are not artefacts of modelling assumptions; they are geometric consequences of how Voronoi cells overlay a density field (Aurenhammer, 1991; Okabe et al., 2000). The resulting maps and numbers have immediate managerial and policy interpretations: for a planner, siting means minimising concentration or access inequality by placing public units where they unlock large pockets of unserved demand; for a manager, the task is to strengthen a focal type while avoiding costly cannibalisation - questions that our index answers with transparent, map-based diagnostics (“who wins where?”; “from whom would a new unit steal?”).

In its baseline form, the spatial HHI is a measure of potential demand under nearest-facility assignment and geometric proximity: it identifies which unit is closest to each location and weights those territorial claims by population density. As such, it does not yet model consumers who deliberately travel further because of price, assortment, quality, brand loyalty, or convenience, nor does it represent households that split purchases across multiple suppliers. The index should be interpreted as a transparent first-order benchmark of spatial access and territorial pressure rather than a full behavioural demand model. A natural extension is to move from potential to effective demand by replacing deterministic nearest-facility assignment with observed trips, credit-card data, loyalty-card data or mobile-location data.

The pipeline is data-light and reproducible. What historically depended on coarse administrative "containers" can now be computed from fine-grained public data: census population grids, address-level points of interest, and open road/building layers (Haklay & Weber, 2008; Statistics Poland, 2023). Where barriers and bridges matter, network distances replace straight-line distances without changing the framework (Boeing, 2017). The Euclidean Voronoi baseline should therefore be interpreted as a spatial benchmark, while settings in which roads, bridges, congestion, travel time or transport mode materially shape accessibility are better represented with network- or travel-time-based distances. In practice: Voronoi assignment → density-weighted shares → two-layer concentration → nested decomposition yields interpretable diagnostics across retail and public services (Fotheringham & O'Kelly, 1989; Huff, 1963).

In sum, we contribute three things. (1) We restore space and density to concentration measurement by defining a spatial HHI that works at unit and type levels and is computable from open data. (2) We provide a nested inter- vs. intra-type decomposition that distinguishes dominance over rivals from internal cannibalisation, giving managers and planners different levers and maps for action. (3) We operationalise siting as an optimisation problem aligned with the index itself, thus linking measurement to decision. The result is a compact, ecology-inspired toolkit for answering what traditional, aspatial indices cannot: who serves whom, and where?

The sHHI index, along with its accompanying location optimisation algorithm, contributes not only to the field of spatial economics but also to the field of decision support systems (DSS) based on geospatial data and ML models (Hu et al., 2025). Because sHHI is density-aware, transparent, and relatively computationally light, it is well-suited for expert systems in three practical arenas. First, in marketing/retail site selection, sHHI can serve as a fast pre-screening signal that highlights catchments with high inter-chain rivalry and flags pockets of intra-chain cannibalisation, improving shortlists before more intensive network or demand-forecasting models are run. Second, for competition-policy analytics, sHHI provides regulators with a spatially explicit market-power diagnostic that complements traditional HHI: the index separates cross-chain rivalry from within-chain concentration, making it easier to identify local dominance and to stress-test merger scenarios on realistic urban geographies. Third, in urban planning of public facilities – primary schools, hospitals, emergency and relief centres - sHHI helps to balance accessibility and redundancy by revealing underserved areas versus saturated ones; the same machinery supports contingency planning under natural-hazard or conflict risk, where resilient coverage matters more than raw capacity. Taken together, these uses position sHHI as a plug-in metric for interactive dashboards and regulatory toolchains, improving explainability and speed while remaining compatible with richer, model-based pipelines.

References

Apparicio, P., Abdelmajid, M., Riva, M., & Shearmur, R. (2008). *Comparing alternative approaches to measuring the geographical accessibility of urban health services: Distance types and aggregation-error issues*. International Journal of Health Geographics, 7, 7. https://doi.org/10.1186/1476-072X-7-7

Aurenhammer, F. (1991). *Voronoi diagrams—A survey of a fundamental geometric data structure*. ACM Computing Surveys, 23(3), 345–405. https://doi.org/10.1145/116873.116880

Baecke, P., & Van den Poel, D. (2012). *Including spatial interdependence in customer acquisition models: A cross-category comparison*. Expert Systems with Applications, 39(15), 12105–12113. https://doi.org/10.1016/j.eswa.2012.04.008

Batty, M. (2013). *The new science of cities*. MIT Press. https://doi.org/10.7551/mitpress/9399.001.0001

Beare, S., & Szakiel, S. (2009). *Spatial competition and the structure of retail markets*. In Proceedings of the 18th World IMACS/MODSIM Congress (Cairns, Australia, 13–17 July 2009). Modelling and Simulation Society of Australia and New Zealand.

Birkin, M., Clarke, G., & Clarke, M. (2002). *Retail geography and intelligent network planning*. Wiley.

Boeing, G. (2017). OSMnx: *New methods for acquiring, constructing, analyzing, and visualizing complex street networks*. Computers, Environment and Urban Systems, 65, 126–139. https://doi.org/10.1016/j.compenvurbsys.2017.05.004

Chen, J., & Chang, Z. (2015). *Rethinking urban green space accessibility: Evaluating and optimizing public transportation system through social network analysis in megacities.* Landscape and Urban Planning, 143, 150–159. https://doi.org/10.1016/j.landurbplan.2015.07.007

Cheddad, A., Mohamad, D., & Abd Manaf, A. (2008). *Exploiting Voronoi diagram properties in face segmentation and features extraction*. Pattern Recognition, 41(12), 3842–3859, https://doi.org/10.1016/j.patcog.2008.06.007

Church, R., & ReVelle, C. (1974). *The maximal covering location problem*. Papers of the Regional Science Association, 32(1), 101–118. https://doi.org/10.1007/BF01942293

Davies, S. (2021). *Competition and concentration: Charting the faultlines* (CCP Working Paper 21-11). Centre for Competition Policy and School of Economics, University of East Anglia.

d'Aspremont, C., Gabszewicz, J. J., & Thisse, J.-F. (1979). On Hotelling's "Stability in Competition." Econometrica, 47(5), 1145–1150. https://doi.org/10.2307/1911955

Ellickson, P. B., Grieco, P. L. E., & Khvastunov, O. (2020). *Measuring competition in spatial retail*. RAND Journal of Economics, 51(1), 189–232. https://doi.org/10.1111/1756-2171.12310

Ewing, R., & Hamidi, S. (2015). *Compactness versus sprawl: A review of recent evidence from the United States*. Journal of Planning Literature, 30(4), 413–432. https://doi.org/10.1177/0885412215595439

Fotheringham, A. S., & O'Kelly, M. E. (1989). *Spatial interaction models: Formulations and applications*. Kluwer Academic.

Hakimi, S. L. (1964). *Optimum locations of switching centers and the absolute centers and medians of a graph*. Operations Research, 12(3), 450–459. https://doi.org/10.1287/opre.12.3.450

Haklay, M., & Weber, P. (2008*). OpenStreetMap: User-generated street maps*. IEEE Pervasive Computing, 7(4), 12–18. https://doi.org/10.1109/MPRV.2008.80

Herfindahl, O. C. (1950). *Concentration in the steel industry* (Doctoral dissertation, Columbia University).

Hirschman, A. O. (1945). *National power and the structure of foreign trade*. University of California Press.

Hotelling, H. (1929). *Stability in competition*. The Economic Journal, 39(153), 41–57. https://doi.org/10.2307/2224214

Hu, H., Tan, D., Thaichon, P., Wang, B., & Zhu, Z. (2025). *Grid-based market sales forecasting for retail businesses using automated machine learning and geospatial intelligence*. Expert Systems with Applications, 284, 127869. https://doi.org/10.1016/j.eswa.2025.127869

Huff, D. L. (1963). *A probabilistic analysis of shopping center trade areas*. Land Economics, 39(1), 81–90. https://doi.org/10.2307/3144521

Kolahdouzan, M. R., & Shahabi, C. (2004). *Voronoi-based k nearest neighbor search for spatial network databases.* In Proceedings of the 30th International Conference on Very Large Data Bases (pp. 840–851). https://doi.org/10.5555/1316689.1316762

Kopczewska, K. (2020). *Applied Spatial Statistics and Econometrics: Data Analysis in R.* Routledge. https://doi.org/10.4324/9781003033219

Kopczewska, K., & Ćwiakowski, P. (2021). *Spatio-temporal stability of housing submarkets: Tracking spatial location of clusters of geographically weighted regression estimates of price determinants.* Land Use Policy, 103, 105292. https://doi.org/10.1016/j.landusepol.2021.105292

Lee, I., & Torpelund-Bruin, C. (2012). *Geographic knowledge discovery from Web map segmentation through generalized Voronoi diagrams*. Expert Systems with Applications, 39(10), 9376–9388. https://doi.org/10.1016/j.eswa.2012.02.129

Lee, I., Torpelund-Bruin, C., & Lee, K. (2012). *Map segmentation for geospatial data mining through generalized higher-order Voronoi diagrams with sequential scan algorithms*. Expert Systems with Applications, 39(12), 11135–11148. https://doi.org/10.1016/j.eswa.2012.03.042

Miura, M., & Shiroishi, H. (2019). *Agent-based modeling and simulation for two-dimensional spatial competition*. In G. Jezic, Y.-H. J. Chen-Burger, R. J. Howlett, L. C. Jain, L. Vlacic, & R. Šperka (Eds.), Agents and Multi-Agent Systems: Technologies and Applications 2018: Proceedings of the 12th International Conference on Agents and Multi-Agent Systems: Technologies and Applications (KES-AMSTA-18) (pp. 67–75). Springer. https://doi.org/10.1007/978-3-319-92031-3_7

Neutens, T., Delafontaine, M., Scott, D. M., & De Maeyer, P. (2012). *An analysis of day-to-day variations in individual space–time accessibility*. Journal of Transport Geography, 23, 81–91. https://doi.org/10.1016/j.jtrangeo.2012.04.001

Okabe, A., Boots, B., Sugihara, K., & Chiu, S. N. (2000). *Spatial tessellations: Concepts and applications of Voronoi diagrams* (2nd ed.). Wiley. https://doi.org/10.1002/9780470317013

Pacala, S. W., & Silander, J. A. (1985). *Neighborhood models of plant population dynamics I: Single-species models of annuals*. The American Naturalist, 125(3), 385–411. https://doi.org/10.1086/284349

Pielou, E. C. (1959). *The use of point-to-plant distances in the study of the pattern of plant populations*. Journal of Ecology, 47(3), 607–613. https://doi.org/10.2307/2257293

Reilly, W. J. (1931). *The law of retail gravitation*. Knickerbocker Press.

Rhoades, S. A. (1993). *The Herfindahl–Hirschman Index*. Federal Reserve Bulletin, 79(3), 188–189.

Roig-Tierno, N., Baviera-Puig, A., Buitrago-Vera, J., & Mas-Verdú, F. (2013). *The retail site location decision process using GIS and the analytical hierarchy process*. Applied Geography, 40, 191–198. https://doi.org/10.1016/j.apgeog.2013.03.005

Salop, S. (1979). *Monopolistic competition with outside goods*. The Bell Journal of Economics, 10(1), 141–156. https://doi.org/10.2307/3003323

Shaffer, S., & Spierdijk, L. (2020). *Measuring multi-product banks' market power using the Lerner index*. Journal of Banking & Finance, 117, 105859. https://doi.org/10.1016/j.jbankfin.2020.105859

Soldatos, G. T. (2021). *Dominant bank oligopoly and economic stability. International Journal of Finance & Economics*, 26(4), 6416–6420. https://doi.org/10.1002/ijfe.2128

Statistics Poland. (2023). *Population grid 2021—Methodology and dataset*. GUS.

Tilman, D. (1988). *Plant strategies and the dynamics and structure of plant communities.* Princeton University Press.

Turolla, S. (2016). *Spatial competition in the French supermarket industry.* Annals of Economics and Statistics/Annales d'Économie et de Statistique, (121/122), 213–259. https://doi.org/10.15609/annaeconstat2009.121-122.213

U.S. Department of Justice & Federal Trade Commission. (2023). *Merger Guidelines.*

van Leeuwen, E., & Lijesen, M. (2012). *Agent-Based Spatial Competition* (ERSA Conference Paper No. ersa12p156). European Regional Science Association.

Wiegand, T., & Moloney, K. A. (2014). *Handbook of spatial point-pattern analysis in ecology.* Chapman & Hall/CRC. https://doi.org/10.1201/b16195

Yu, W. (2016). *Spatial co-location pattern mining for location-based services in road networks.* Expert Systems with Applications, 46, 324–335. https://doi.org/10.1016/j.eswa.2015.10.010

Zhang, J., & Robinson, D. T. (2022). *Investigating path dependence and spatial characteristics for retail success using location allocation and agent-based approaches*. Computers, Environment and Urban Systems, 94, 101798. https://doi.org/10.1016/j.compenvurbsys.2022.101798

Zhong, Z., Zheng, L., Kang, G., Li, S., & Yang, Y. (2020). *Random erasing data augmentation.* AAAI Conference on Artificial Intelligence, 34(7), 13001–13008. https://doi.org/10.1609/aaai.v34i07.7000

APPENDIX

Appendix A. Algorithmic details for Section 2.3

Appendix A gives the single-type version of the siting algorithm. This is the case used when all facilities belong to one operator or one public-service system, such as public primary schools or a single retail chain considered in isolation. Because there is only one type, there is no inter-type rivalry. The relevant objective is outlet-level spatial concentration.

Let X be the current set of units and let $\mathcal{Y}$ be the feasible set of candidate locations. The population grid is G, with cell populations P_g and density-weighted demand P_g^{η}. Total weighted demand is:

$$W_\eta = \sum_{g \in G} P_g^{\eta}.$$

Under the nearest-facility rule, each cell g is currently served by unit $j(g)$. The spatial share of unit j is:

$$s_j = \frac{\sum_{g:j(g)=j} P_g^{\eta}}{W_\eta}.$$

The single-type spatial HHI is therefore:

$$sHHI = H_{\text{outlet}} = \sum_{j \in X} s_j^2.$$

When a candidate $y \in \mathcal{Y}$ is added, it wins the cells for which it is closer than the current assigned unit:

$$W_{\text{win}}(y) = \{g \in G: d(g,y) < d(g, x_{j(g)})\}.$$

The new candidate's share is:

$$s_y{}' = \frac{\sum_{g \in W_{\text{win}}(y)} P_g^{\eta}}{W_\eta}.$$

Each affected existing unit j loses the mass of its cells that switch to y:

$$s_j{}' = s_j - \frac{\sum_{\substack{g \in W_{\text{win}}(y) \\ j(g)=j}} P_g^{\eta}}{W_\eta}.$$

Unaffected units keep $s_j{}' = s_j$. The updated concentration is:

$$sHHI'(y) = \sum_{j \in X} \left(s_j{}'\right)^2 + \left(s_y{}'\right)^2.$$

The best single candidate is:

$$y^\star = \operatorname*{argmin}_{y \in \mathcal{Y}} sHHI'(y).$$

For a public provider, this means reducing inequality of assigned demand across facilities. For a single retail chain, it should be interpreted as internal load balancing rather than full profit maximisation, because no rival demand is present in the single-type model.

Algorithm 2. Greedy siting under intra-type competition

Input:

1. X: current units, all belonging to one type.
2. G: population grid with cell populations P_g.
3. Y: feasible candidate sites.
4. m: number of units to add.
5. η: density-weighting parameter.

Initialise:

1. Compute W_η = sum_{g in G} P_g^η.
2. Assign each cell g to its nearest current unit j(g).
3. Compute baseline shares s_j and baseline sHHI = Σ_j s_j².

Procedure:

For k = 1, …, m:

1. Set best_site = none and best_value = +∞.
2. For each candidate y in Y:
   a. compute W_win(y);
   b. compute the candidate share s_y′;
   c. update affected existing shares s_j′;
   d. compute sHHI_new(y) = sum_{j in X}(s_j')^2 + (s_y')^2;
   e. if sHHI′(y) < best_value, set best_value = sHHI′(y) and best_site = y.
3. Accept the best site.

Acceptance step:

Add best_site to X, remove best_site from Y, reassign the cells in W_win(best_site), and update the affected shares locally.

Output: the augmented set X with m new units and the final outlet-level spatial HHI.

This algorithm is the single-type special case of the general optimisation in Appendix B. In the notation of Section 3, if there is only one type, $H_{\text{inter}} = 1$ and $NSCI_{\alpha} = \alpha + (1-\alpha)H_{\text{outlet}}$. Since α is constant, minimising $NSCI_{\alpha}$ is equivalent to minimising H_{outlet}.

Appendix B. Algorithmic details for Section 3.3

Appendix B gives the multi-type siting algorithm. It covers cases with several chains, operators or service formats and therefore distinguishes between planner and manager objectives.

Notation

Let X be the current set of units, partitioned into types T. Let $\mathcal{Y}$ be the set of feasible candidate sites. Let G be the population grid, with cell populations P_g and density-weighted demand P_g^{η}. Total weighted demand is:

$$W_{\eta} = \sum_{g \in G} P_g^{\eta}.$$

For each current assignment, the outlet share is:

$$s_j = \frac{\sum_{g:j(g)=j} P_g^{\eta}}{W_{\eta}}.$$

For each type t, the type share is:

$$S_t = \sum_{j \in J_t} s_j.$$

Within-type concentration is:

$$I_t = \sum_{j \in J_t} \left(\frac{s_j}{S_t}\right)^2, \qquad S_t > 0.$$

The two global concentration layers are:

$$H_{\text{inter}} = \sum_{t \in T} S_t^2,$$

and:

$$H_{\text{outlet}} = \sum_{j \in X} s_j^2 = \sum_{t \in T} S_t^2 \, I_t.$$

The planner objective is:

$$NSCI_{\alpha} = \alpha H_{\text{inter}} + (1 - \alpha) H_{\text{outlet}}.$$

For a focal type τ, the manager objective evaluates a candidate y by decomposing the cells it wins:

$$W_{\text{win}}(y) = \{g \in G: d(g, y) < d(g, x_{j(g)})\}.$$

Demand captured from rival types is:

$$A_\tau(y) = \sum_{\substack{g \in W_{\text{win}}(y) \\ type(j(g)) \neq \tau}} P_g^\eta,$$

and demand reallocated from the focal type's own outlets is:

$$B_\tau(y) = \sum_{\substack{g \in W_{\text{win}}(y) \\ type(j(g)) = \tau}} P_g^\eta.$$

The manager's score is:

$$M_\kappa(\tau; y) = \frac{A_\tau(y)}{W_\eta} - \kappa \frac{B_\tau(y)}{W_\eta}.$$

Algorithm 3. Greedy siting with inter- and intra-type competition

Input:

1. X: current units with type labels.
2. G: grid cells with population counts P_g.
3. Y: feasible candidate sites.
4. m: number of sites to add.
5. η: density-weighting parameter.
6. α: NSCI inter/outlet mixing weight.
7. κ: manager penalty for self-cannibalisation.
8. objective: either planner(system) or manager(τ).

Initialise:

1. Compute W_η = sum_{g in G} P_g^η.
2. Assign each cell g to its nearest current unit j(g).
3. Compute baseline s_j, S_t, I_t, H_inter, H_outlet and NSCI_α.
4. Cache, for each cell g, its current owner j(g), distance d(g, x_{j(g)}), and owner type.

Planner branch:

For k = 1, …, m:

1. Set best_site = none and best_value = +∞.
2. For each candidate y in Y:
   a. compute W_win(y);
   b. update the shares of the candidate and affected existing units;
   c. recompute affected type shares S_t′ and within-type terms I_t′;
   d. compute value(y) = α sum_t(S_t')^2 + (1 - α) sum_t(S_t')^2 I_t';
   e. if value(y) < best_value, set best_value = value(y) and best_site = y.
3. Accept best_site, update assignments locally, and remove it from Y.

Manager branch:

For k = 1, …, m:

1. Set best_site = none and best_score = −∞.
2. For each candidate y in Y:

a. compute W_win(y);
b. compute A_τ(y) and B_τ(y);
c. compute score(y) = A_τ(y)/W_η − κB_τ(y)/W_η;
d. if score(y) > best_score, set best_score = score(y) and best_site = y.
3. Accept best_site, update assignments locally, and remove it from Y.

Optional local improvement:
After the greedy additions, try one-for-one swaps between selected new sites and nearby feasible candidates. Accept a swap if it improves the relevant objective: lower NSCI_α for the planner, or higher M_κ for the manager. Repeat until no improving swap exists.

Output: the augmented set X with m new sites and the final objective value.

The two branches deliberately answer different economic questions. The planner branch asks where new facilities should be placed to reduce system-wide spatial concentration and improve access balance. The manager branch asks where a focal chain should expand to win rival demand while limiting self-cannibalisation. Both branches use the same density-weighted spatial assignment and therefore remain internally consistent with the sHHI and NSCI definitions in Section 3.

SUPPLEMENT

All datasets and code are hosted in our public GitHub repository (https://github.com/Endote/spatial-HHI/tree/master). We provide: (i) fully annotated R scripts for Sections 2 and 3 that simulate index behaviour under controlled scenarios; (ii) a complete OpenStreetMap acquisition pipeline (downloading POI and boundaries, cleaning, and constructing population-weighted Voronoi catchments) to compute sHHI, decompose inter- vs. intra-type components, and visualise maps and diagnostics; and (iii) siting optimisation code (greedy + local swaps) with case studies spanning retail formats (Żabka, Lidl, Biedronka) and public facilities (schools). Repository folders mirror the manuscript, specifying inputs, outputs, and exact commands to regenerate the figures and tables. In parallel, we release a Shiny application that reproduces the Section 2–3 simulations online, enabling interactive sensitivity checks and scenario analysis (https://microeconomics.shinyapps.io/sHHI/).

Table of Contents

Dictionary

HHI - Herfindahl-Hirschman Index
sHHI - Spatial Herfindahl-Hirschman Index
NSCI - Nested Spatial Competition Index
OSM - OpenStreetMap
POI - Points of Interest
NSP - Narodowy Spis Powszechny
JEL - Journal of Economic Literature classification

Table of Figures

Table of Appendices